



## Characterization and application of three novel biosorbents “*Eucalyptus globulus*, *Cynara cardunculus*, and *Prunus cerasifera*” to dye removal

Aoumria Ouldoumouma<sup>a,b</sup>, Laurence Reinert<sup>c</sup>, Nouredine Benderdouche<sup>b,\*</sup>, Benaouda Bestani<sup>b</sup>, Laurent Duclaux<sup>c</sup>

<sup>a</sup>LRSBG, Faculté des Sciences et de la Technologie, Université de Mascara BP 763, Route Mamounia Mascara 29000, Algeria

<sup>b</sup>LSEA2M, Faculté des Sciences et de la Technologie, Université de Mostaganem, B.P. 188, Mostaganem 27000, Algeria

Tel. +213(0)772618906; Fax: +21345206476; email: benderdouchen@yahoo.fr

<sup>c</sup>LCME, Université de Savoie, Le Bourget du Lac Cedex 73376, France

Received 28 April 2012; Accepted 29 October 2012

### ABSTRACT

Three biosorbents: *Eucalyptus globulus*, *Cynara cardunculus*, and *Prunus cerasifera* leaves were tested to remove Methylene Blue from aqueous solutions. The three biosorbents were characterized by the determination of the Methylene Blue accessible surface, iodine number, BET specific surface area using nitrogen adsorption at 77K, morphological analysis by scanning electron microscopy,  $pH_{PZC}$ , and FTIR analysis. The Methylene Blue adsorption uptakes of the biosorbents were studied as a function of pH, biosorbent dose, stirring speed, ionic strength, and contact time. Optimal conditions for maximum removal of Methylene Blue were found to be: a pH of 10, an adsorbent dose of  $8\text{ g L}^{-1}$ , and a contact time of 2 h for *E. globulus* and *C. cardunculus*, and a pH of 6.5, an adsorbent dose of  $4\text{ g L}^{-1}$  and a contact time of 2 h for *P. cerasifera*. The Langmuir models as determined from batch experiments yielded a maximum capacity of adsorption by biosorbent prepared from *E. globulus* leaves of  $250\text{ mg g}^{-1}$  against  $333\text{ mg g}^{-1}$  and  $143\text{ mg g}^{-1}$  for biosorbents prepared from *C. cardunculus* and *P. cerasifera* leaves, respectively. For all the materials used, the adsorption process was found exothermic and spontaneous.

**Keywords:** Biosorption; *Eucalyptus globulus*; *Cynara cardunculus*; *Prunus cerasifera*; Methylene Blue

### 1. Introduction

Water becomes increasingly scarce and its quality is constantly deteriorating. The World Health Organization (WHO) considers that 80% of diseases that affect the world's population are directly borne by water [1]. Effluents from textile industries are part of wastewater. Synthetic dyes today are a relatively large

group of chemical compounds found in all spheres of daily life. They are considered dangerous pollutants because they are toxic to aquatic life, mutagenic and carcinogenic, and can affect vital organs of man. Some colorant effluents are resistant to oxidants and do not biodegrade easily [2,3].

The world production of dyes is estimated at 700,000 tons/year of which 140,000 are released into effluents during the various stages of implementation

\*Corresponding author.

and preparation. The exact behavior of dyes in the environment is often unknown. These discharges, especially dyes, can be toxic to most organisms [2], hence it is desirable to remove dyes from wastewater not only because they constitute visible pollution and are resented as such but also because of their effect on living organisms and health in human beings. Various physicochemical techniques have been used to treat wastewater with varying success including membrane techniques, distillation, coagulation–flocculation, advanced oxidation processes, and adsorption. Among these techniques, adsorption has proved to be a remarkable economic and efficient process especially for poor developing countries where scarcity of water necessitates the use of low-cost methods to recycle wastewater.

Many researchers have studied the use of plants to extract heavy metals from water and soil [4]. Some plant species have shown a remarkable uptake of certain metals such as copper, zinc, and lead [5,6]. Several studies were conducted to prepare adsorbents from waste plants for pollutants removal [7–9]. Recently, several researchers have investigated dye removal from aqueous solution using agricultural wastes or natural materials. Various low-cost adsorbents such as wood [10], coir pith [11], sugar industry mud [12], and plum kernels [13] have been examined. We focused our work on the use of three untreated plants, namely, cardoon (*Cynara cardunculus*), prune (*Prunus cerasifera*), and eucalyptus (*Eucalyptus globulus*), designated respectively as CARD, PRUN, and EUCA, for the removal of a typical dye, Methylene Blue, which was selected as a model molecule to study the adsorption properties of the biosorbents. We have characterized, and compared the performance of adsorption using UV–VIS spectrometry.

## 2. Materials and methods

### 2.1. Biosorbents preparation

The biosorbents used are the leaves of cardoon, prune, and eucalyptus from the region of Mascara (Algeria) due to their abundance in this area. They were washed with laboratory-produced distilled water ( $5 \mu\text{S}/\text{cm}$ ) and dried in an oven at  $60^\circ\text{C}$  for 24 h. Then, they were ball-milled at 90 revolutions per minute for 30 min, using a CrosschopVierzen grinder, and sieved to obtain particle diameter lower than 0.071 mm (212 mesh).

### 2.2. Adsorbate

The adsorbate used was analytical grade Methylene Blue (MB) having a molecular weight of

$319.86 \text{ g mol}^{-1}$  and a dye content  $\geq 85\%$  supplied by the Merck company. MB was chosen for this study because of its known strong adsorption onto solids. Distilled water was used to prepare all the solutions and reagents. The chemical structure of the MB dye is depicted in Fig. 1.

### 2.3. Iodine test

Iodine number is a widely used parameter for activated carbon testing for its simplicity and a rapid assessment of adsorbent quality. It gives an estimate of its surface area and porosity. The iodine number is defined as the milligrams of iodine adsorbed by one gram of material when the iodine residual concentration of the filtrate is 0.02 N ( $0.01 \text{ mol L}^{-1}$ ) according to ASTM D4607 (1999) standard [14], which is based on a three-point isotherm. A standard iodine solution (0.1 N) is treated with three different weights of biosorbent. The sample is treated with 10 mL of 5% (V/V) HCl. The mixture is boiled for 30 s and then cooled at room temperature. 100 mL of 0.1 N iodine solution is immediately added to the mixture and stirred for 30 s. The solution is then filtered and 50 mL of the filtrate is titrated with 0.1 N ( $0.05 \text{ mol L}^{-1}$ ) sodium thiosulphate solution using thyodene (or starch) as an indicator. The amount of iodine adsorbed per gram of biosorbent is plotted against the residual iodine concentration, using logarithmic axes. If the residual iodine concentration is not within the range (0.008–0.04 N), the procedure is repeated using different carbon masses for each isotherm point. A regression analysis is applied to the three points and the iodine number is calculated as the amount adsorbed at a residual iodine concentration of 0.02 N.

### 2.4. pH of zero point charge ( $\text{pH}_{\text{PZC}}$ )

The  $\text{pH}_{\text{PZC}}$  is defined as the pH for which there is neutral charge on the surface of the adsorbent. A volume (50 mL) of sodium chloride solution ( $0.01 \text{ mol L}^{-1}$ ) was placed in capped bottles and the pH was adjusted from 2 to 12 by adding concentrated sodium hydroxide or hydrochloric acid. A 0.15 g of biosorbent was then added to the NaCl solutions. After stirring magnetically

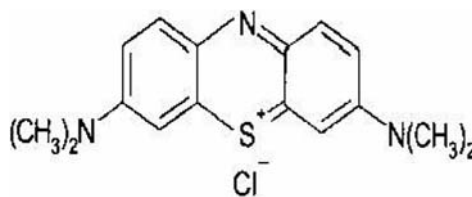


Fig. 1. Structure of Methylene Blue.

for 48 h, the final pH was measured and plotted against the initial pH. The pH corresponding to the point of intersection with the pH (final) = pH (initial) was taken as the  $\text{pH}_{\text{PZC}}$  of the material.

### 2.5. Determination of the surface area accessible to Methylene Blue

Methylene Blue is a typical dye used to calculate the accessible surface of sorbents to large molecules. The available surface with Methylene Blue is calculated by the following equation:

$$S_{\text{MB}} = \frac{b \cdot N \cdot S}{M} \quad (1)$$

with  $S_{\text{MB}}$  is the surface area ( $\text{m}^2 \text{g}^{-1}$ ),  $b$  is maximum adsorption capacity ( $\text{mg g}^{-1}$ ) based on a monolayer coverage. It can be determined from the Langmuir model,  $N$  is Avogadro's number ( $6.023 \times 10^{23} \text{ mol}^{-1}$ ),  $S$  is the surface occupied by a molecule of Methylene Blue (taken as  $119 \text{ \AA}^2$ ), and  $M$  is the molecular weight of Methylene Blue ( $319.86 \text{ g mol}^{-1}$ ).

### 2.6. $\text{N}_2$ adsorption–desorption at 77 K

The  $\text{N}_2$  adsorption–desorption isotherms of the biosorbents were measured using an automatic adsorption instrument (ASAP 2000, Micromeritics, France) [15] at liquid nitrogen temperature (77 K). Prior to measurements, biosorbent samples were degassed at  $80^\circ\text{C}$  for 12 h under vacuum. The specific surface areas ( $S_{\text{BET}}$ ) of the biosorbents were calculated using the BET (Brunauer–Emmett–Teller) equation by assuming the area of the nitrogen molecule to be  $16.2 \text{ \AA}^2$ . The total pore volumes were estimated as the liquid volume of adsorbate adsorbed ( $\text{N}_2$ ) at a relative pressure of 0.99 [15].

### 2.7. Infrared spectroscopy

Mid-infrared transmittance measurements of the adsorbents studied were carried out on a NICOLET 380 FT-IR spectrometer at room temperature in the  $400\text{--}4000 \text{ cm}^{-1}$  wavenumber range, with a  $2 \text{ cm}^{-1}$  resolution. Pellets made of a mixture of 0.6 mg of biosorbent, and 200 mg of KBr were pressed at 350 MPa, and oven-dried for 48 h at  $110^\circ\text{C}$  before analysis.

### 2.8. Thermogravimetric analysis

Changes in the mass of biosorbents during decomposition and loss of volatile material that occurred

upon heating were followed by thermogravimetry. Thermogravimetric analyses were performed in a Pyrox furnace coupled to a Mettler balance. Analyses were performed under air, from room temperature to  $1000^\circ\text{C}$  with a heating rate of  $4^\circ\text{C min}^{-1}$ . Temperature and mass data were collected and processed by a computer dedicated to the system.

### 2.9. Morphological analysis

Morphological analysis on biosorbents surface was carried out by Scanning Electron Microscopy (SEM) using a LEO Stereoscan 440 microscope in the secondary electron mode, coupled with an energy dispersive spectrometer (EDS, Kevex Sigma).

### 2.10. Methylene Blue adsorption experiments

#### 2.10.1. Effect of pH

A 25 mL of Methylene Blue solution of known concentration were successively introduced into a series of beakers containing each a mass of biosorbent (EUCA, PRUN, or CARD); the pH value was adjusted to 2, 4, 8, 10, and 11 with  $1 \text{ mol L}^{-1}$  sodium hydroxide and hydrochloric acid. The mixture was stirred for a specified period, then filtered and analyzed by spectrophotometry.

#### 2.10.2. Effect of adsorbent dose

The effect of the adsorbent dose was studied by varying the adsorbent amounts from 4 to  $16 \text{ g L}^{-1}$  for the initial MB concentration of  $100 \text{ mg L}^{-1}$  (at pH of MB).

#### 2.10.3. Effect of stirring speed

To check the effect of stirring speed on mass transfer toward the surface of biosorbent, various stirring speeds ( $w = 500, 700, 900, 1100 \text{ rpm}$ ) were investigated.

#### 2.10.4. Effect of contact time and kinetics

A 25 mL of initial Methylene Blue solutions of concentration  $100 \text{ mg L}^{-1}$  were mixed with 0.1 g of each biosorbent used. The effect of contact time was determined for 5, 15, 30, 50, 60, 90, 120, and 180 min at a pH of 6.5 which is the initial MB solution pH. The results obtained were plotted graphically as the percentage of MB removed with time ( $t$ ) according to the following equation:

$$(C_0 - C_{eq})/C_0 = f \quad (2)$$

$C_0$  and  $C_{eq}$  represent the initial and the equilibrium concentration, respectively ( $\text{mg L}^{-1}$ ).

### 2.10.5. Isothermal adsorption of Methylene Blue

The adsorption process was studied under the established optimal conditions determined for the three biosorbents. To establish the adsorption isotherms of Methylene Blue onto the three biosorbents, concentrations of MB ranging from 30 to 2200  $\text{mg L}^{-1}$  were used for all subsequent handlings. After an equilibrium contact time determined from kinetic tests, the solutions were filtered and then analyzed. The uptake of Methylene Blue at equilibrium  $q_e$  ( $\text{mg g}^{-1}$ ) on the surface of biosorbent was calculated by the following equation:

$$q_e = \frac{(C_0 - C_{eq}) \cdot V}{m} \quad (3)$$

where  $m$  is the mass of the biosorbent used (g) and  $V$  is the volume of solution (mL).

## 3. Results and discussion

### 3.1. Characterization of biosorbents used

The iodine number,  $\text{pH}_{\text{PZC}}$  and BET specific surface area are shown in Table 1 for the three biosorbents.

Table 1  
Characterization of the studied biosorbents

	EUCA	CARD	PRUN
Iodine number ( $\text{mg g}^{-1}$ )	446	535	370
$\text{pH}_{\text{PZC}}$	6.37	6.25	6.80
$S_{\text{BET}}$ ( $\text{m}^2 \text{g}^{-1}$ )	14.0	22.0	13.8

Table 1 shows that the iodine number values were highest for CARD ( $535 \text{ mg g}^{-1}$ ) followed by EUCA ( $446 \text{ mg g}^{-1}$ ) and by PRUN ( $370 \text{ mg g}^{-1}$ ). The  $\text{pH}_{\text{PZC}}$  values are very similar for all the biosorbents and closed to 6.5, indicating that these natural materials can be considered as close to neutral adsorbents.

The BET surface area is highest for CARD in accordance with the iodine number values whilst those for the other two biosorbents are close.

#### 3.1.1. FTIR analysis

Fig. 2 shows the Fourier-transform infrared spectra of the three biosorbents. The broad absorption band at

$3300\text{--}3600 \text{ cm}^{-1}$  with a maximum at about  $3400 \text{ cm}^{-1}$  is characteristic of the stretching vibration of hydrogen-bonded hydroxyl groups (from water).

The FTIR spectrum of the biosorbent shows bands at  $2935 \text{ cm}^{-1}$  and  $2800 \text{ cm}^{-1}$  arising from aliphatic C–H stretching (in an aromatic methoxyl group, in methyl and methylene groups of side chains) and from aromatic C–H stretching, respectively. The broad band observed in all spectra at  $\sim 1044.2 \text{ cm}^{-1}$  (Fig. 1) can be assigned to C–O stretching in acids, alcohols, phenols, ethers, and/or esters groups [16]. The dominant peaks observed at  $512$  and  $659 \text{ cm}^{-1}$  suggest the presence of C–H rocking vibrations of cellulose. In the region  $1300\text{--}1400 \text{ cm}^{-1}$ , several absorption bands corresponding to stretching vibrations of C–N bonds are observed. A peak observed at  $1626 \text{ cm}^{-1}$  corresponds to bending vibrations in the plane of H bonds. The band located at  $1830 \text{ cm}^{-1}$  indicates the presence of C–O.

#### 3.1.2. SEM analysis

The Scanning Electron Microscopy (SEM) images of the three biosorbents prepared show relatively heterogeneous non-porous surfaces as shown in Fig. 3. The SEM images of the surfaces indicate that the particles were mainly arranged in layers. They have a cotton-wool aspect.

#### 3.1.3. Thermogravimetric analysis

The thermograms were done on the three materials to study their stability to temperature in order to assess the degassing range for BET analysis and to have information about the carbonization behavior for any subsequent treatment. They presented a first weight loss at low temperature ( $T < 100^\circ\text{C}$ ) attributed to the elimination of adsorbed water. It corresponds to about 10% for CARD and to about 5% for the two other biosorbents. The first mass loss was attributed to the departure of physisorbed water and the second loss at  $\sim 100^\circ\text{C}$ , ( $100 < T < 150^\circ\text{C}$ ) to the emission of chemisorbed water. The first stage of carbonization occurs in the temperature range of  $200\text{--}500^\circ\text{C}$  (70% loss) due to the eradication of volatile material rich in functional groups (lignin, hemicellulose, and cellulose).

After characterization of the biosorbents used with respect to EUCA, CARD and PRUN, the next section deals with dye adsorption results.

## 3.2. Adsorption results

### 3.2.1. Effect of dose of adsorbent

The effect of adsorption dose on the removal of MB showed that significant removal percents were

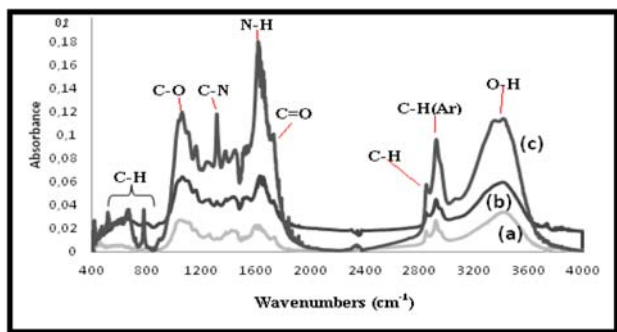


Fig. 2. FTIR spectra of the three biosorbents: (a) EUCA, (b) CARD, and (c) PRUN.

obtained at a minimum dose of  $8 \text{ g L}^{-1}$  for EUCA, and CARD and at a minimum of  $4 \text{ g L}^{-1}$  for PRUN.

The percentage of MB increased initially very rapidly with the increase of adsorbent content. As the adsorbent dose increases, the number of adsorbent particles increases thus, more MB is attached to their surfaces. Beyond an adsorbent content of  $4 \text{ g L}^{-1}$ , the percentage of MB removed reached a constant value. A slight increase in uptake was observed when the dose was increased from 4 to  $8 \text{ g L}^{-1}$ . Any further addition of the adsorbent beyond this value did not cause any significant change in the adsorption.

### 3.2.2. Effect of pH on the adsorption uptake of biosorbents

Many studies showed that pH is an important factor in determining the potential for adsorption of cationic and anionic organic compounds [17–19]. The results of adsorption uptake of MB as a function of pH are shown in Fig. 4.

It can be observed that increasing the pH of the solution leads to a better elimination of the dye. The best rate of biosorption takes place at an optimum pH of 10 for EUCA and CARD, and at  $\text{pH} = 6.5$  for PRUN. Results from the FTIR analyses indicate that the three biosorbents consist of various functional groups such as hydroxyl ( $-\text{OH}$ ) and carbonyl ( $-\text{CO}$ ) that may be influenced by the pH. The  $\text{pK}_a$  of MB is 0.04 [20]; hence, MB is completely ionized at a pH greater than 0.04 and exists under a cationic form [21]. At a pH higher than  $\text{pH}_{\text{ZPC}}$ , the charge at the surface of adsorbent changes and becomes negative, causing a higher electrostatic attraction of the cationic dyes, leading to an increase of the adsorption of ions  $\text{OH}$ -Methylene Blue [22]. A decrease was observed at  $\text{pH} = 4$  and 2 which can be explained by the fact that at low pH values, there is an electrostatic repulsion between the cations and the biosorbent surface positively charged. When the pH increases, the MB cation can replace ion

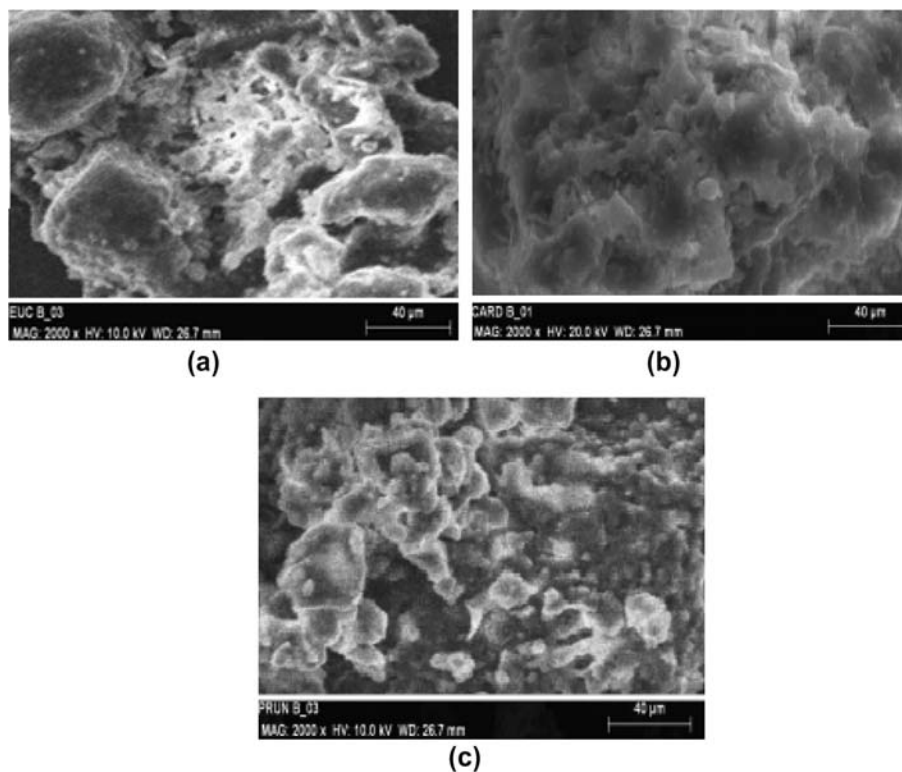


Fig. 3. Scanning electron micrographs of the biosorbents: (a) EUCA, (b) CARD, and (c) PRUN.

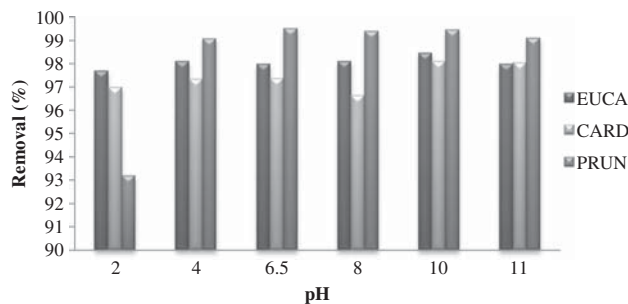


Fig. 4. Effect of pH on biosorption with  $C_0 = 100 \text{ mg L}^{-1}$ .

on the biosorbent surface, leading to an increase of the adsorption by ion exchange mechanism [22]. The lowest adsorption of MB at acidic conditions can be attributed in part to the presence of excess of  $\text{H}^+$  ions destabilizing the basic dye and competing with cationic dye ions for the adsorption sites [17–19]. Studies conducted by Ray-Castro and Lodeiro [23] showed that algae-based systems with a negative charge possess high affinity for cations. The adsorption could be explained by pure electrostatic interactions between the negatively charged biosorbent and the positive charge of Methylene Blue [23]. The dye adsorption capacity depends both on the properties of the adsorbent surface and on the structure of the dye [24,25].

### 3.2.3. Effect of stirring speed on the kinetics of adsorption by biosorbents

In an adsorption system in batch mode, the stirring speed plays a very important role to ensure a good distribution of the adsorbent in the total volume of the adsorbate [26]. According to the series of experiments performed on the three biosorbents (EUCA, CARD, and PRUN), it was found that the maximum removal of Methylene Blue remains unchanged when increasing the stirring speed. These results can be explained by a very rapid spread of adsorbate and a rapid diffusion of the dye through the biosorbents. They are consistent with the work published by Weng et al. [21]. In other words, the diffusion of the MB ion from the solution to the surface of the three materials and into the pores occurred quickly and easily. Since the uptake of MB was not significantly influenced by agitation, a stirring speed of 500 rpm was therefore used for all further experiments.

### 3.2.4. Effect of contact time and kinetics

Fig. 5 shows that the adsorption equilibrium was reached after a contact time of 120 min.

To investigate the controlling mechanism and the reaction order of the adsorption of Methylene Blue

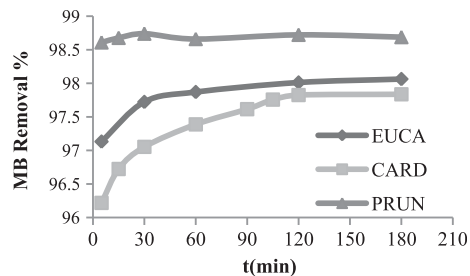


Fig. 5. Percentage of MB removed vs. time for the three biosorbents ( $C_0 = 100 \text{ mg L}^{-1}$ ).

onto the three materials prepared, the Lagergren pseudo-first order and pseudo-second order equations, and the intra-particle diffusion model were applied. The pseudo-first order rate equation is given as:

$$\log(q_e - q_t) = \log q_e - (k_1/2.303)t \quad (4)$$

where  $q_t$  and  $q_e$  are the adsorption capacities at time  $t$  and at equilibrium ( $\text{mg g}^{-1}$ ) respectively, and  $k_1$  ( $\text{min}^{-1}$ ) is the rate constant of the pseudo-first order adsorption. Linear plots of  $\log(q_e - q_t)$  against  $t$  give access to the rate constants  $k_1$ . The pseudo-second-order equation can be expressed as:

$$\frac{t}{q_t} = \frac{1}{k_2 q_e^2} + \frac{1}{q_e} t \quad (5)$$

where  $k_2$  is the pseudo-second order rate constant ( $\text{mg g}^{-1} \text{ min}^{-1}$ ).  $k_2 q_e^2$  can be assumed as the initial adsorption rate as  $t$  goes to zero. The plot of  $t/q_t$  vs.  $t$  gives a straight line if second order kinetics describes the biosorption process (Fig. 6).

The intra-particle diffusion model can be expressed as follows:

$$q_t = K_{int} t^{1/2} + C \quad (6)$$

where  $K_{int}$  ( $\text{mg g}^{-1} \text{ min}^{-1/2}$ ) is the intra-particle diffusion rate constant and  $C$  ( $\text{mg g}^{-1}$ ) is the intercept. The value of  $C$  gives an idea about the thickness of the boundary layer: the larger the intercept, the greater the boundary-layer effect. The plots  $q_t$  vs.  $t^{1/2}$  for the two concentrations (100 and  $200 \text{ mg L}^{-1}$ ) are shown in Fig. 7.

The nature of the plots reveals the existence of two distinct portions which are different for the three biosorbents for both solute concentrations. The first portions may be attributed to boundary layer (or film) diffusion effects. The three biosorbents behave differently in these initial stages as EUCA shows a more

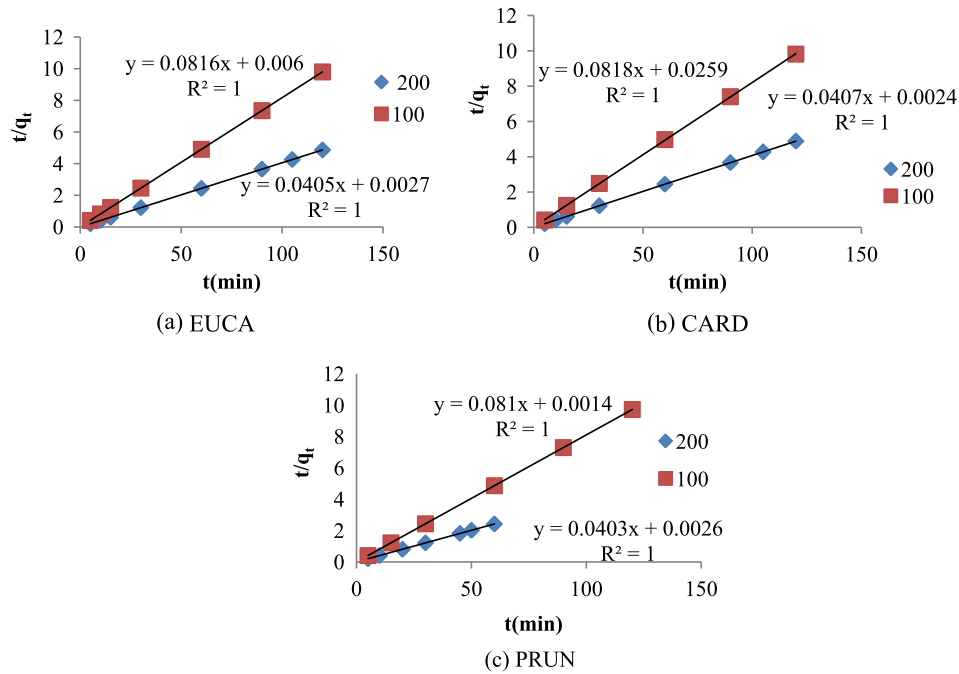


Fig. 6. Pseudo-second order kinetic models for the biosorption of MB by the three biosorbents: (a) EUCA, (b) CARD, and (c) PRUN—initial concentrations of 100 and 200 mg L<sup>-1</sup>.

curved portion for the 100 mg L<sup>-1</sup> concentration whereas CARD behaves so for the 200 mg L<sup>-1</sup> concentration but for PRUN the curvature is less apparent. All the plots deviate from origin, indicating a difference between the rate of mass transfer in the initial and final stages of biosorption, and that intra-particle diffusion is not the sole rate-limiting step.

The computed constants (experimental and calculated values) that have a direct correlation with the adsorption speed are reported in Table 2.

The sum of squares error (SSE, %) is one method which has been used in literature to test the validity of each model. The sum of squares error is given as:

$$SSE(\%) = \sqrt{\sum \frac{[(q_e)_{exp} - (q_e)_{cal}]^2}{N}} \quad (7)$$

where  $N$  is the number of data points.

The generally low values of regression coefficient ( $R^2$ ) of the first-order kinetic model for CARD and PRUN for the two concentrations used (100 and 200 mg L<sup>-1</sup>) suggest that this model does not describe their adsorption kinetics. The adsorption capacities confirm this conclusion, since the calculated values do not correspond to those found experimentally. For EUCA, however, for a concentration of 100 mg L<sup>-1</sup> and CARD for a concentration of 200 mg L<sup>-1</sup> fair correlation coefficients were obtained but the calculated adsorption capacities still do not correspond to the experimental ones, which means kinetics are not true first order and the parameter  $k_1 (q_e - q_t)$  does not represent the number of available sites. The kinetic models were further tested using the SSE (sum of squares error) as computed using Eq. (7). It can be seen that the SSE (%) values are lower for the second-order

Table 2  
Pseudo-second order model kinetic data for Methylene Blue adsorption

	$q_e$ (exp) (mg g <sup>-1</sup> )	$q_e$ (calc) (mg g <sup>-1</sup> )	$k_2$ (g/mg min)	$h$ (mg/g min)	$R^2$	SSE (%)
EUCA (100 mg L <sup>-1</sup> )	12.252	12.255	1.111	166.67	1	0.002
EUCA (200 mg L <sup>-1</sup> )	24.658	24.691	0.608	371.73	1	0.023
CARD (100 mg L <sup>-1</sup> )	12.227	12.225	0.259	38.610	1	0.001
CARD (200 mg L <sup>-1</sup> )	24.572	24.570	0.690	416.667	1	0.001
PRUN (100 mg L <sup>-1</sup> )	12.343	12.346	4.690	714.286	1	0.001
PRUN (200 mg L <sup>-1</sup> )	24.812	24.814	0.625	384.615	1	0.002

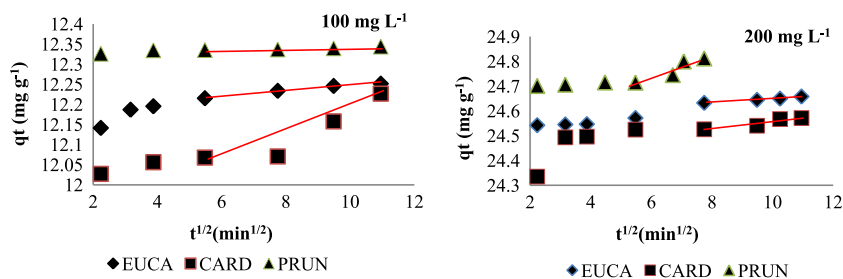


Fig. 7. Intra-particle diffusion of MB by the three biosorbents EUCA (■), CARD (◆), and PRUN (▲).

kinetic model (0.002 to 0.023%) with respect to those for the pseudo-order first model (8.488 to 17.293%), which confirms the better applicability of the pseudo-second order model (Table 2).

The diffusion rate of intra-particle has two stages as shown in Fig. 7; the first step can be attributed to the rapid spread of the adsorbent with the solution on the outer surface of the adsorbent (plateau). This step is followed by a plateau-like step (phase 2) that can be attributed to the final stage of equilibrium.

The linear variation of  $q_e$  vs.  $t^{1/2}$  shows that internal diffusion can also control the adsorption process [27].

From Table 3, the constant  $C$  was found to increase with increase of MB concentration for the three biosorbents EUCA, CARD and PRUN, indicating an increase of the thickness of the boundary layer [28].

Although the fair  $R^2$  values given in Table 3 indicate that the intra-particle diffusion process may be involved even though the intra-particle diffusion rate constant,  $K_{int}$ , are low for the three systems, the best model to fit the adsorption kinetics of the three biosorbents is the pseudo-second order model.

### 3.2.5. Determination of adsorption isotherm of Methylene Blue

The linearized Langmuir and Freundlich models' adsorption isotherms were used to reproduce the adsorption isotherms of Methylene Blue by the ground biosorbent leaves

$$\frac{C_{eq}}{q} = \frac{1}{b}C_{eq} + \frac{1}{K_L b} \quad (8)$$

where  $q$  is the amount of dye adsorbed per gram of adsorbent (mg g<sup>-1</sup>),  $C_{eq}$  is the concentration of dye at equilibrium (mg L<sup>-1</sup>).  $K_L$  and  $b$  are the Langmuir constants related to adsorption energy and maximum capacity for monolayer coverage, respectively.

$$\log q = \frac{1}{n} \log C_{eq} + \log K_F \quad (9)$$

$K_F$  and  $n$  are the Freundlich constants.

Equilibrium adsorption data of Methylene Blue onto the three biosorbents studied are shown in Fig. 8.

Fig. 8 clearly shows different adsorption capacities for the three biosorbents. The linearized forms of the Langmuir and the Freundlich models give correlation coefficients in the range 0.97–0.99 (Table 4). The Freundlich model is not in good agreement with the isotherm profiles. Despite the profile is Langmuirian for the isotherms; the MB cannot be adsorbed on a monolayer because the BET Surface area is very low compared to the surface area occupied by MB.

Table 5 summarizes the values of maximum adsorption capacity of Methylene Blue by biosorbents at optimum pH and temperature. The Langmuir constants for the two biosorbents, EUCA and CARD adsorption uptake give values of 250 mg g<sup>-1</sup> and 333 mg g<sup>-1</sup>, respectively, and 143 mg g<sup>-1</sup> for PRUN,

Table 3  
Intra-particle diffusion constants

	$K_{int}$ (mg g <sup>-1</sup> min <sup>-1/2</sup> )	$C$	$R^2$
EUCA (100 mg L <sup>-1</sup> )	0.007	12.18	0.98
EUCA (200 mg L <sup>-1</sup> )	0.008	24.57	0.98
CARD (100 mg L <sup>-1</sup> )	0.030	11.88	0.85
CARD (200 mg L <sup>-1</sup> )	0.015	24.41	0.91
PRUN (100 mg L <sup>-1</sup> )	0.002	12.33	0.90
PRUN (200 mg L <sup>-1</sup> )	0.005	24.69	0.89

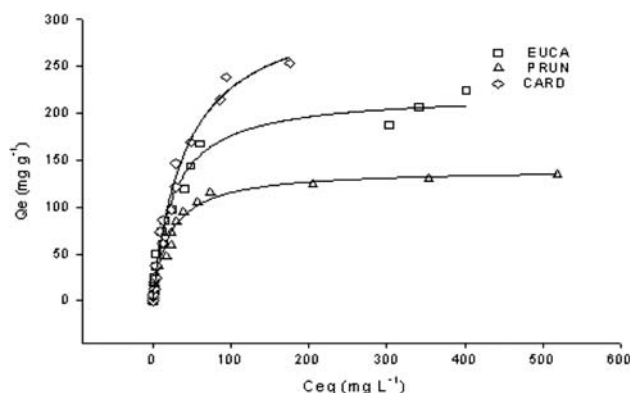


Fig. 8. Isothermal adsorption of MB by the three biosorbents (EUCA (□), CARD (◇), PRUN (△), solid line = Langmuir fit).

which shows that these biosorbents already performed well, though no treatment was imposed on them. The results compare competitively with some published

results [7,8,29–31]. This may provide an advantage for developing countries local economies to use such low-cost adsorbents.

### 3.2.6. Surface area accessible to Methylene Blue

Table 6 gives the Methylene Blue accessible surface and the ratio of BET surface area and MB accessible surface. By comparing the different determined parameters, it is clear that the surface accessible to MB is very large compared to the BET surface area. Similar results were found by He and Tebo, Rubin et al., and Sassi et al. [33–35].

This suggests that the adsorption of MB may be multilayered as the volumes of MB adsorbed (taking  $1.43 \times 0.61 \times 0.40 \text{ nm}^3$  as the volume occupied by one MB molecule) by CARD, EUCA, and PRUN: 0.21, 0.16 and  $0.94 \text{ cm}^3 \text{ g}^{-1}$ , respectively, are much lower than the corresponding total pore volumes as estimated

Table 4  
Results of adsorption isotherms of Methylene Blue, according to the Langmuir and Freundlich models

	EUCA	CARD	PRUN
<i>Langmuir model</i>			
Equation	$y = 0.004x + 0.123$	$y = 0.003x + 0.141$	$y = 0.007x + 0.121$
$b \text{ (mg g}^{-1}\text{)}$	250	333	143
$K_2 \text{ (L mg}^{-1}\text{)}$	0.032	0.021	0.058
$R^2$	0.99	0.97	0.99
<i>Freundlich model</i>			
Equation	$y = 0.567x + 2.49$	$y = 0.777x + 2.081$	$y = 0.430x + 1.159$
$n$	0.40	0.48	0.86
$K_F$	1.75	2.16	1.54
$R^2$	0.86	0.95	0.91

Table 5  
Maximum capacities for adsorption of Methylene Blue by some adsorbents

Adsorbent	Maximum adsorption capacity (mg g <sup>-1</sup> )	Reference
Activated carbon prepared from olive stone	556.6	[7]
Activated carbon	373.9	[15]
Biosorbent <i>Cynara cardunculus</i> (CARD)	333	This study
Bio-adsorbent pineapple leaf powder	296.83	[22]
<i>Sargassum mutucum</i> seaweed	279.2	[23]
Biosorbent <i>Eucalyptus globulus</i> (EUCA)	250	This study
Cotton waste	240	[24]
<i>Hydrilla verticillata</i>	198	[25]
Moss	185	[26]
Peanut hull	161.3	[32]
Activated carbon prepared by <i>Salsola</i>	153.84	[8]
Biosorbent <i>Prunus cerasefera</i> (PRUN)	143	This study

Table 6

Comparison between BET surface area and area accessible to Methylene Blue

	EUCA	CARD	PRUN
Volume of MB adsorbed ( $\text{cm}^3 \text{g}^{-1}$ )	0.16	0.21	0.94
Surface area accessible to MB ( $\text{m}^2 \text{g}^{-1}$ )	560	746	320
Total pore volumes ( $\text{cm}^3 \text{g}^{-1}$ ) at 0.99 relative pressure	6.29	10.22	4.48
$S_{\text{BET}}/S_{\text{MB}}$	0.025	0.029	0.043

from the liquid volumes of adsorbed nitrogen at a relative pressure of 0.99: 10.22, 6.29, and  $4.48 \text{ cm}^3 \text{g}^{-1}$ , respectively.

### 3.2.7. Effect of ionic strength on the kinetics of adsorption by biosorbents

The presence of ions may affect the performance of the biosorption process [36,37]. The influence of the ionic strength on the adsorption of Methylene Blue by the three biosorbents was studied using solutions of NaCl from 0 to  $0.1 \text{ mol L}^{-1}$ . Fig. 9(a–c) presents the effect of ionic strength on the removal of MB. For the three biosorbents, sorption potential decreases with the increase of the ionic strength. The effect of ionic strength on dye removal would indicate that adsorbent–adsorbate electrostatic forces are of attractive nature [38]. Several authors [22,39] found similar results.

### 3.2.8. Thermodynamic parameters

Adsorption isotherms were studied at four different temperatures in the range 298–318 K in order to determine the thermodynamic parameters ( $\Delta G^\circ$ ,  $\Delta S^\circ$ , and  $\Delta H^\circ$ ) of the adsorption process.

The free energy change ( $\Delta G^\circ$ ) was calculated from the following equation [40]:

$$\Delta G^\circ = -RT \ln Kd \quad (10)$$

where  $R$  ( $8.314 \text{ J mol}^{-1} \text{ K}^{-1}$ ) is the ideal gas constant,  $T$  is the temperature in Kelvin, and  $Kd$  is the distribution coefficient calculated from the following equation [40]:

$$Kd = \frac{C_{\text{eqs}}}{C_{\text{EQ}}} \quad (11)$$

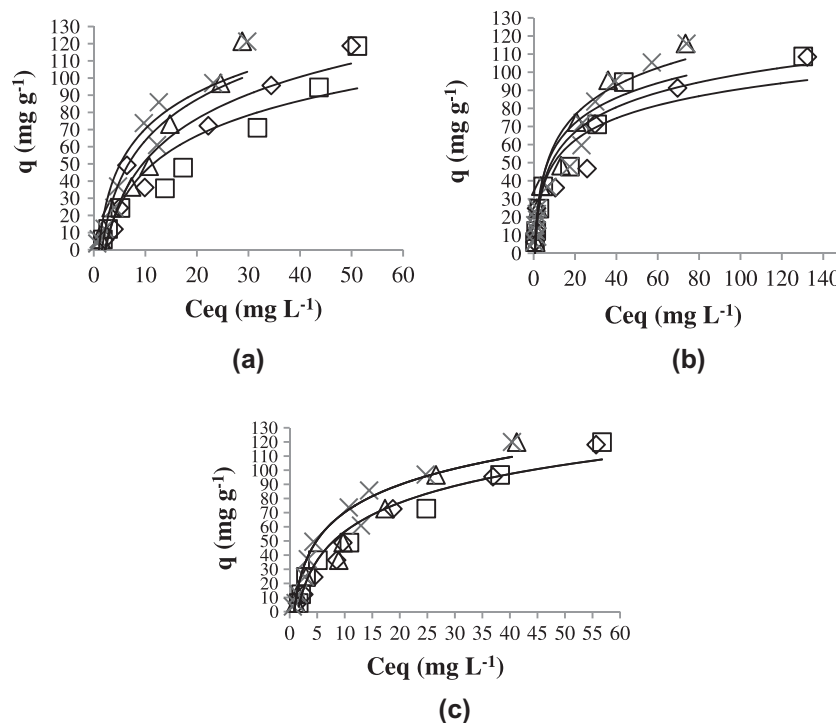


Fig. 9. Effect of ionic strength ( $[\text{NaCl}]$ :  $0 \text{ mol L}^{-1}$  ( $\times$ ),  $0.001 \text{ mol L}^{-1}$  ( $\Delta$ ),  $0.01 \text{ mol L}^{-1}$  ( $\square$ ),  $0.1 \text{ mol L}^{-1}$  ( $\diamond$ )) on the isothermal elimination of MB by the biosorbent EUCA (a), CARD (b), and PRUN (c).

Table 7  
Some thermodynamic parameters calculated from the Langmuir isotherms

Adsorbent	$\Delta G^\circ$ (kJ/mol)				$\Delta H^\circ$ (kJ/mol)	$\Delta S^\circ$ (kJ/mol K)
	Temperature (K)					
	298	308	313	318		
EUCA	–	–5.51	–5.44	–5.26	–13.26	–0.025
CARD	–	–4.71	–4.69	–4.61	–7.76	–0.01
PRUN	–6.5	–6.33	–5.97	–	–16.86	–0.034

where  $C_{eqs}$  is the amount of dye (mg) adsorbed on the adsorbent per liter of the solution at equilibrium and  $C_{EQ}$  is the equilibrium concentration ( $\text{mg L}^{-1}$ ) of the dye in the solution. The Van't Hoff equation (Eq. (12)) [41] was used to calculate the enthalpy and entropy changes:

$$\ln Kd = \frac{\Delta S^\circ}{R} - \frac{\Delta H^\circ}{RT} \quad (12)$$

Table 7 summarizes the values of the thermodynamic parameters calculated from the Langmuir isotherms.

Low negative values of  $\Delta H^\circ$  indicate that the adsorption is physical involving weak attractive forces and is exothermic. This implies that the adsorption process is energetically stable. The weakly negative values of  $\Delta H^\circ$  imply loose bonding between the MB molecules and the three biosorbents surface [42]. Negative values of  $\Delta S^\circ$  show an ordering of the adsorbed phase at the surface of adsorbent throughout the adsorption process. Negative values of  $\Delta G^\circ$  indicate that adsorption is spontaneous and that there is a great affinity between Methylene Blue and the biosorbents. The same observations were reported for the adsorption of MB by other authors [22,43–45].

#### 4. Conclusion

This work was devoted to the study of the removal of Methylene Blue by three biosorbents abundantly available in Algeria. The biosorbents characterization of EUCA, PRUN, and CARD showed that the surface calculated for the MB ( $560$ ,  $320$ , and  $746 \text{ m}^2 \text{ g}^{-1}$ ) was very large compared to the BET surface area ( $14$ ,  $13.8$ , and  $22 \text{ m}^2 \text{ g}^{-1}$ , respectively). It was found that each gram of EUCA, PRUN, and CARD leaves adsorbed  $250$ ,  $143$ , and  $333 \text{ mg}$  of MB, respectively, at an optimum pH of  $10$  for EUCA and CARD and  $6.5$  for PRUN. The adsorption isotherms obey the Langmuir equation with a very rapid initial step and reach equilibrium within  $120 \text{ min}$ . The pseudo-second

order kinetic model is the most adapted to describe the adsorption process. The FTIR studies pointed out the presence of different surface groups (amino groups, carboxyl, and hydroxyl groups), that chemically interact with MB cations and thus play an important role in the adsorption process.

The adsorption of MB on the three biosorbents is spontaneous and exothermic, indicating a physisorption phenomenon. This study shows that biosorbents are excellent example of economic use of plant waste for the protection of the environment without any inconvenience. Because of their abundance, these natural resources are effective and alternative biomass for the removal of dyes from aqueous solutions with promising use in industrial processes.

#### References

- [1] Y. Akria, R.M. David, E. Philip, in: Proc. 21st Mid-Atlantic Conf. Ind. Waste, Harrisburg, PA, June 26–27, Technomic, Lancaster, PA, USA, 1989.
- [2] R. Perrin, J.P. Scharff, Chimie industrielle, 2ème ed., Dunod, Paris, 1999.
- [3] A.S. Ozcan, A. Ozcan, Adsorption of acid dyes from aqueous solutions onto acid-activated bentonite, J. Colloid Interface Sci. 276 (2004) 39–46.
- [4] N. Fiol, I. Villaescusa, M. Martinez, N. Miralles, J. Poch, J. Serarols, Sorption of Pb(II), Ni(II), Cu(II) and Cd(II) from aqueous solution by olive stone waste, Sep. Purif. Technol. 50 (2006) 132–140.
- [5] X.S. Wang, Z.Z. Li, C. Sun, Removal of Cr(VI) from aqueous solutions by low-cost biosorbents: marine macroalgae and agricultural by-products, J. Hazard. Mater. 153 (2008) 1176–1184.
- [6] V. Singh, Removal of lead from aqueous solutions using *Cassia grandis* seed gumgraft-poly(methylmethacrylate), J. Colloid Interface Sci. 316 (2007) 224–232.
- [7] M. Termoul, B. Bestani, N. Benderdouche, M. Belhakem, E. Naffrechoux, Removal of phenol and 4-chlorophenol from aqueous solutions by olive stone-based activated carbon, J. Sci. Technol. 24(5) (2006) 375–387.
- [8] B. Bestani, N. Benderdouche, B. Benstaali, A. Addou, Adsorption of methylene blue and iodine from aqueous solutions by a desert *Salsola vermiculata* species, Bioresour. Technol. 99 (2008) 8441–8444.
- [9] N. Benderdouche, B. Bestani, B. Benstaali, D. Derriche, Enhancement of the adsorptive properties of a desert *Salsola vermiculata* species, J. Adsorpt. Sci. Technol. 21(8) (2003) 739–750.

- [10] H. Asfour, O. Fadali, M. Nassar, M. El-Feundi, Equilibrium studies on adsorption of basic dyes on hard wood, *J. Chem. Technol. Biotechnol.* 35 (1985) 21–27.
- [11] C. Namasivayam, R. Radhika, S. Suba, Uptake of dyes by a promising locally available agricultural solid waste: coir pith, *Waste Manage.* 21 (2001) 381–387.
- [12] Y. Magdy, A. Daifullah, Adsorption of a basic dye from aqueous solutions onto sugar-industry-mud in two modes of operations, *Waste Manage.* 18 (1998) 219–226.
- [13] R. Juang, F. Wu, R. Tseng, Mechanism of adsorption of dyes and phenols from water using activated carbons prepared from plum kernels, *J. Colloid Interface Sci.* 227 (2000) 437–444.
- [14] ASTM, Standard Test Method for Determination of Iodine Number of Activated Carbon, vol. 4, section 15, ASTM Annual Book, 1999, pp. 4607–46948.
- [15] J. Jagiello, J.P. Olivier, A simple two-dimensional NLDFT model of gas adsorption in finite carbon pores, application to pore structure analysis, *J. Phys. Chem.* 113 (2009) 19382–19385.
- [16] J. Zawadzki, Infrared spectroscopy in surface chemistry of ethylene, In: P.A. Thrower (Ed), *Chemistry and Physics of Carbon*, vol. 21, Marcel Dekker, New York, NY, pp. 147–386, 1989.
- [17] P. Waranusantigul, P. Pokethitiyook, M. Kruatrachue, E.S. Upatham, Kinetics of basic dye (methylene blue) biosorption by giant duckweed (*Spirodela polyrrhiza*), *Environ. Pollut.* 125 (2003) 385–392.
- [18] S. Gao, S. Tanada, I. Abe, M. Kitagawa, Y. Matsubara, Adsorption of organic compounds on surface-modified activated carbon in aqueous solution, *Soc. Activated Carbon Res. Osaka (Japan)* 163 (1994) 138–144.
- [19] K.G. Bhattacharyya, A. Sharma, Kinetics and thermodynamics of methylene blue on nee, (*Azadirachta indica*) leaf powder, *Dyes Pigm.* 65 (2005) 51–59.
- [20] A. Albert, E.P. Sergeant, *Ionization Constants of Acids and Bases. A Laboratory Manual*, Wiley, New York, NY, 1962.
- [21] C-H. Weng, Y-T. Lin, T-W. Tzeng, Removal of Methylene blue from aqueous solution by adsorption onto pineapple leaf powder, *J. of Haz. Mater* (2009) 417–424.
- [22] A. Seco, P. Marzal, C. Gabaldon, Study of the adsorption of Cd and Zn onto an activated carbon: influence on pH, cation concentration, and adsorbent concentration, *Sep. Sci. Technol.* 34 (1999) 1577–1593.
- [23] C. Rey-Castro, P. Lodeiro, Acid–base properties of brown seaweed biomass considered as a Donnan gel. A model reflecting electrostatic effects and chemical heterogeneity, *Environ. Sci. Technol.* 37 (2003) 5159–5167.
- [24] J.X. Lin, S.L. Zhan, M.H. Fang, X.Q. Qian, H. Yang, Adsorption of basic dye from aqueous solution onto fly ash, *J. Environ. Manage.* 87 (2008) 193–200.
- [25] S.D. Khattria, M.K. Singh, Removal of malachite green from dye wastewater using neem sawdust by adsorption, *J. Hazard. Mater.* 167 (2009) 1089–1094.
- [26] G. Crini, H.N. Peindy, F. Ginber, C. Robert, Removal of C. I basic green 4 (malachite green) from aqueous solutions by adsorption using cyclodextrin-based adsorbent: kinetic and equilibrium studies, *Sep. Purif. Technol.* 53 (2007) 97–110.
- [27] M.C. Ncibi, B. Mahjoub, M. Seffen, Kinetic and equilibrium studies of methylene blue biosorption by *Posidonia oceanica* (L.) fibres, *J. Hazard. Mater.* 139 (2007) 280–285.
- [28] H. Zhi-jun, W. Nan-xi, T. Jun, C. Jian-qiu, Z. Wen-ying, Kinetic and equilibrium of cefradine adsorption onto peanut husk, *Desalination Water Treat.* 37 (2012) 160–168.
- [29] E. Rubin, P. Rodriguez, R. Herrero, J. Cremades, I. Barbara, M.E.S. De Vicente, Removal of methylene blue from aqueous solutions using as biosorbent *Sargassum muticum*: an invasive macroalga in Europe, *J. Chem. Technol. Biotechnol.* 80 (2004) 291–298.
- [30] K.S. Low, C.K. Lee, L.L. Heng, Sorption of basic dyes by *Hydrilla verticillata*, *Environ. Technol.* 14 (1993) 115–124.
- [31] K.S. Low, C.K. Lee, K.K. Tan, Biosorption of basic dyes by water hyacinth roots, *Bioresour. Technol.* 52 (1995) 79–83.
- [32] D. Ozer, G.D. Dursan, A. Ozer, Methylene blue adsorption from aqueous solutions by dehydrated peanut hull, *J. Hazard. Mater.* 144 (2007) 171–179.
- [33] L.M. He, B.M. Tebo, Surface charge properties of and Cu(II) adsorption by spores of the marine *Bacillus* sp. strain sg-1, *Appl. Environ. Microbiol.* 64 (1998) 1123–1129.
- [34] E. Rubin, P. Rodriguez, R. Herrero, J. Cremades, I. Barbara, M.E.S.d. Vicente, Removal of methylene blue from aqueous solutions using as biosorbent *Sargassum muticum*: an invasive macroalga in Europe, *J. Chem. Technol. Biotechnol.* 80 (2005) 291–298.
- [35] M. Sassi, B. Bestani, A. Hadj Said, N. Benderdouche, E. Guibal, Removal of heavy metal ions from aqueous solutions by a local dairy sludge as a biosorbent, *Desalination* 262 (2010) 243–250.
- [36] B. Greene, R. McPherson, D. Darvall, Algal sorbents for selective metal ions recovery, In: W. Patterson, R. Pasino (Eds), *Metal Speciation, Separation and Recovery*, Lewis, Chelsea, MI, pp. 315–338, 2000.
- [37] G.J. Ramelow, D. Fralick, Y. Zhao, Factors affecting the uptake of aqueous metal ions by dried sea weed biomass, *Microbios* 72 (1992) 81–93.
- [38] J. German-Heins, M. Flury, Sorption of brilliant blue FCF in soils as affected by pH and ionic strength, *Geoderma* 97 (2000) 87–101.
- [39] N.S. Maurya, A.K. Mittal, P. Cornel, E. Rother, Biosorption of dyes using dead macro fungi: effect of dye structure, ionic strength and pH, *Bioresour. Technol.* 97 (2006) 512–521.
- [40] K.K. Panday, P. Gup, V.N. Singh, Copper (II) removal from aqueous solutions by fly-ash, *Water Res.* 7 (1985) 869–875.
- [41] W.J. Weber, A.M. Morris, Kinetics of adsorption on carbon from solution, *Div. Am. Soc. Civ. Eng.* 89 (1963) 31–59.
- [42] F. Ferrero, Dye removal by low cost adsorbents hazelnut shells in comparison with wood sawdust, *J. Hazard. Mater.* 142 (2007) 144–152.
- [43] F.A. Pavan Flavio, A.C. Mazzocato, Y. Gushikem, Removal of methylene blue dye from aqueous solutions by adsorption using yellow passion fruit peel as adsorbent, *Bioresour. Technol.* 99 (2008) 3162–3165.
- [44] B.H. Hameed, A.T.M. Din, A.L. Ahmad, Adsorption of methylene blue onto bamboo-based activated carbon: kinetics and equilibrium studies, *J. Hazard. Mater.* 141 (2007) 819–825.
- [45] B.H. Hameed, A.L. Ahmad, K.N.A. Latiff, Adsorption of basic dye (methylene blue) onto activated carbon prepared from rattan sawdust, *Dyes Pigm.* 75 (2007) 143–149.